ResearchGate

See discussions, stats, and author profiles for this publication at: https://www.researchgate.net/publication/243749564

Crossover from Nearest-Neighbor Hopping Conduction to Efros-Shklovskii Variable-Range Hopping Conduction in Hydrogenated Amorphous Silicon Films

Article *in* Japanese Journal of Applied Physics · November 2009

DOI: 10.1143/JJAP.48.111203

CITATIONS
55

READS
1,566

4 authors, including:

Necmi Serin
Ankara University
70 PUBLICATIONS **1,376** CITATIONS

SEE PROFILE

Tülay Serin
Ankara University
92 PUBLICATIONS **1,767** CITATIONS

SEE PROFILE

Mesut Kasap
Çanakkale Onsekiz Mart Üniversitesi
61 PUBLICATIONS **917** CITATIONS

SEE PROFILE

Some of the authors of this publication are also working on these related projects:

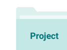
Influence of oxygen flow rate in CuO View project

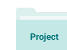
Pure and stable metallic phase molybdenum disulfide nanosheets for hydrogen evolution reaction View project

All content following this page was uploaded by Abdullah Yildiz on 14 February 2015.

The user has requested enhancement of the downloaded file.

Reprinted from

JAPANESE JOURNAL OF
APPLIED
PHYSICS

REGULAR PAPER

Crossover from Nearest-Neighbor Hopping Conduction to Efros–Shklovskii Variable-Range Hopping Conduction in Hydrogenated Amorphous Silicon Films

Abdullah Yildiz, Necmi Serin, Tülay Serin, and Mehmet Kasap

Jpn. J. Appl. Phys. **48** (2009) 111203

© 2009 The Japan Society of Applied Physics

Person-to-person distribution (up to 10 persons) by the author only. Not permitted for publication for institutional repositories or on personal Web sites.

Japanese Journal of Applied Physics **48** (2009) 111203 **REGULAR PAPER**

Crossover from Nearest-Neighbor Hopping Conduction to Efros–Shklovskii Variable-Range Hopping Conduction in Hydrogenated Amorphous Silicon Films

Abdullah Yildiz[1,2*], Necmi Serin[1], Tülay Serin[1], and Mehmet Kasap[3]

[1] *Department of Engineering Physics, Faculty of Engineering, Ankara University, 06100 Ankara, Turkey*
[2] *Department of Physics, Faculty of Science and Arts, Ahi Evran University, 40040 Kirsehir, Turkey*
[3] *Department of Physics, Faculty of Science and Arts, Gazi University, Teknikokular, 06500 Ankara, Turkey*

Received June 3, 2009; revised August 11, 2009; accepted August 27, 2009; published online November 20, 2009

We presented the results of optical and electrical studies of the properties of hydrogenated amorphous silicon (a-Si:H) film which was prepared by hot wire method. Using transmittance measurements, the dielectric constant of the a-Si:H was determined. The temperature-dependent conductivity was measured using the two-point probe method in the temperature range 115–326 K. It was shown that the temperature-dependent conductivity can be well explained by the nearest-neighbor hopping conduction and the Efros–Shklovskii variable-range hopping conduction models. A clear transition from the nearest-neighbor hopping conduction mechanism to the Efros–Shklovskii variable-range hopping conduction mechanism was also observed. The transition between two conduction regimes and characteristic hopping temperatures, as well as the complete set of parameters describing the properties of the localized electrons (the localization length, the hopping energy, the hopping distance, the width of the Coulomb gap, and the value of the density of states at the Fermi level) were determined. © 2009 The Japan Society of Applied Physics

DOI: 10.1143/JJAP.48.111203

1. Introduction

The electronic transport properties of amorphous silicon (a-Si:H) is of considerable interest owing to the many applications under development that rely crucially on its conductivity. The a-Si:H is important for electronic devices such as image sensors and thin-film transistors.[1,2]

There is a considerable interest to achieve a deeper understanding of transport in disordered semiconductors. In disordered semiconductors, charge carrier transport becomes dominated by hopping between defect states relatively close to the Fermi level at sufficiently low temperatures.[3,4] To understand the localization of electronic states, temperature dependence of conductivity data of amorphous silicon and related alloys have been analyzed with the help of various hopping models.[5–9] In the amorphous silicon, the electron conduction paths are composed of s-p hybrid orbitals and carrier transport is controlled by the nearest-neighbor hopping (NNH) or the variable-range hopping (VRH) conduction.[10] In this material, it was typically found that the activation energy of the electrical conductivity decreases progressively as the temperature falls.[5–9] This indicates that the conduction is controlled by the VRH conduction at low temperatures.

Many studies have been devoted to the characterization of amorphous silicon and related alloys. However, no work providing a detailed explanation for the crossover from the NNH to the Efros–Shklovskii (ES) VRH in a-Si:H as temperature decreases has been presented to date. On the other hand, a transition from simple thermally activated conduction to the Mott VRH was observed as temperature decreases in amorphous silicon structures.[6] Yakimov *et al.*[8] revealed the crossover at reduced temperatures from the ES VRH to simple thermally activated conduction in amorphous $Si_{1-x}Mn_x$ films. This unusual behavior was attributed to the presence of a "hard" magnetic gap in amorphous $Si_{1-x}Mn_x$ films.

In this work, the optical and electrical properties of undoped a-Si:H film are investigated by means of the transmittance and electrical conductivity. The temperature-dependent conductivity of this film is explained in terms of hopping conductivity. A clear crossover between the NNH conduction and the ES VRH conduction is observed at about 220 K.

2. Experimental Procedure

Undoped a-Si:H film is grown under condition $T_{Fil} = 1300\,°C$, $C_H = 14.23$ on the glass substrate by hot wire technique with coated chromium metal electrode. Here, C_H is defined as the ratio of H_2 hydrogen flow rate to the silane SiH_4 flow rate. In order to provide the electrical conductivity, the second chromium metal contact is applied on undoped a-Si:H film under a vacuum of 1×10^{-7} Torr and a Cr/a-Si:H/Cr sandwich structure is fabricated. The sample is placed on the fiber holder as shown in Fig. 1. The concentration N_d of a-Si:H film is determined as $9.6 \times 10^{16}\,cm^{-3}$ by means of Hall measurement, as the Hall carrier concentration at room temperature can be assumed almost equal to donor concentration. The dielectric constant of and the thickness of the a-Si:H film, d, are determined from the optical measurement by using Sloan-Dektak 3030 profile meter. Urbach energy E_{rb}, and E_{Tauc} are determined from the optical ultraviolet–visible (UV–vis) transmittance measurement. The values of d, E_{rb}, and E_{Tauc} are determined as 1.94 μm, 58.3 meV, and 1.67 eV, respectively.

The electrical conductivity of the film is determined by the two-point probe method in the temperature range 115–326 K. The current passing through the Cr/a-Si:H/Cr sandwich structure is measured by means of computer controlled Keithley's 228 voltage/current meter. The electrical conductivity of the film for various temperatures is determined from the current–temperature characteristics. A constant voltage (100 V) is applied between the two probes on the film and the change in current with respect to the change in temperature of the film is measured by using an amperemeter. High quality silver paste is used for the contacts to minimize the contact resistance (Fig. 1). The electrical conductivity, σ is calculated using the relationship $\sigma = L/(RA)$, where L, R, and A are the length, resistance, and cross section, respectively.

*E-mail address: yildizab@gazi.edu.tr

 © 2009 The Japan Society of Applied Physics

Person-to-person distribution (up to 10 persons) by the author only. Not permitted for publication for institutional repositories or on personal Web sites.

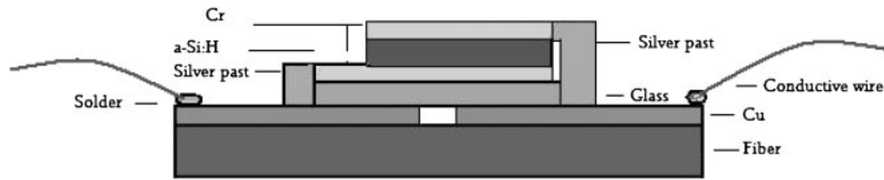

Fig. 1. Cr/a-Si:H/Cr sandwich structure, used for the electrical conductivity measurement of a-Si:H thin film.

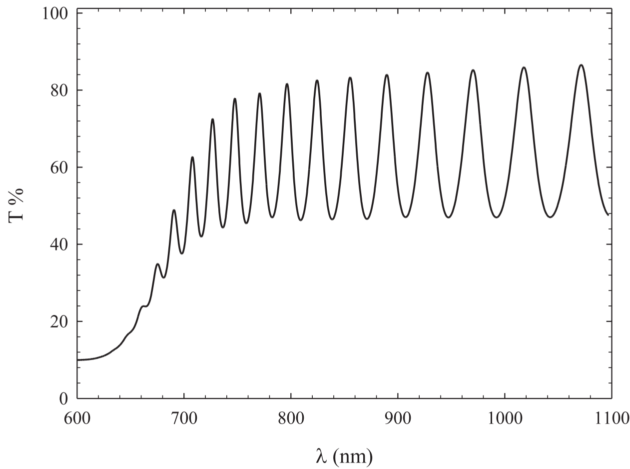

Fig. 2. Typical transmission spectra as a function of the wavelength for a-Si:H film.

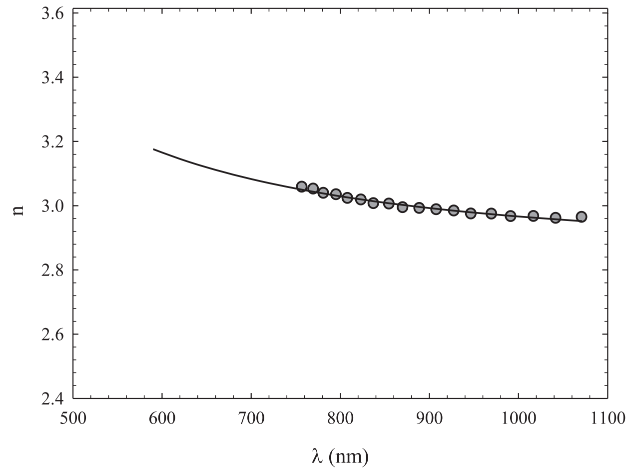

Fig. 3. Refractive index vs the wavelength for a-Si:H film.

3. Results and Discussion

Figure 2 shows the typical transmission spectra of the film in the wavelength range 600–1100 nm. It is clear from Fig. 2 that the interference effects disappear in the region of very strong absorption, while the maximum amplitude is obtained in the transparent region, where the envelope method[11] can be applied more accurately. Complex refractive index of the film is $n_c = n - ik$, where n is the refractive index and $k = \alpha\lambda/4\pi$ is the extinction coefficient. In the region of weak and medium absorption, the real part of the refractive index, n, can be calculated using the equation:

$$n = [N + (N^2 - n_s^2)^{1/2}]^{1/2}, \quad (1)$$

where

$$N = 2n_s \frac{T_M - T_m}{T_M T_m} + \frac{n_s^2 + 1}{2}. \quad (2)$$

Here, n_s is the refractive index of the substrate that is determined experimentally and equals to $n_s = 1.51$, T_M and T_m are determined from the extremes of the interference strings at any desired wavelength.

Figure 3 shows the refractive index versus the wavelength for the film. It is observed that the refractive index is slowly varying function of wavelength and decreases with the increase in wavelength of the incident light. In order to find the refractive index in the region of strong absorption, where the interferences disappear, we can fit the experimental values of n to a reasonable function such as a two-term Cauchy dispersion relation $n = A + B/\lambda^2$. Figure 3 shows the experimental and calculated values of refractive index and they agree closely.

The dependence of the complex refractive index, n_c, on the lattice dielectric constant, ε, is given by[12]

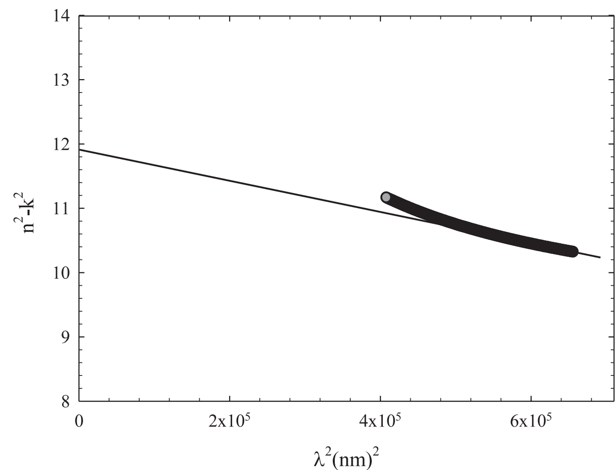

Fig. 4. Plot of $n^2 - k^2$ vs λ^2 for a-Si:H film.

$$n^2 - k^2 = \varepsilon - \left(\frac{e^2}{\pi c^2}\right)\left(\frac{N}{m^*}\right)\lambda^2, \quad (3)$$

where N is the carrier concentration, m^* is the effective mass, c is the speed of light, and e is the electronic charge. The plot of $n^2 - k^2$ versus λ^2 is shown in Fig. 4. The value of ε is deduced from the extrapolation of this plot to $\lambda^2 = 0$ and it is obtained as 11.9. This is in perfectly agreement with the generally accepted value of ε.[13,14)]

To establish the dominant conduction mechanism in the film, the electrical conductivity has been measured from 115 to 326 K. Figure 5 shows the Arrhenius plot ($\ln\sigma$ vs $1000/T$) for the film. As seen from the Fig. 5, no single law conduction can fit the entire curve of the conductivity. The plot suggests that there are two types of conduction mechanisms contributing to the conductivity in different

 © 2009 The Japan Society of Applied Physics

Person-to-person distribution (up to 10 persons) by the author only. Not permitted for publication for institutional repositories or on personal Web sites.

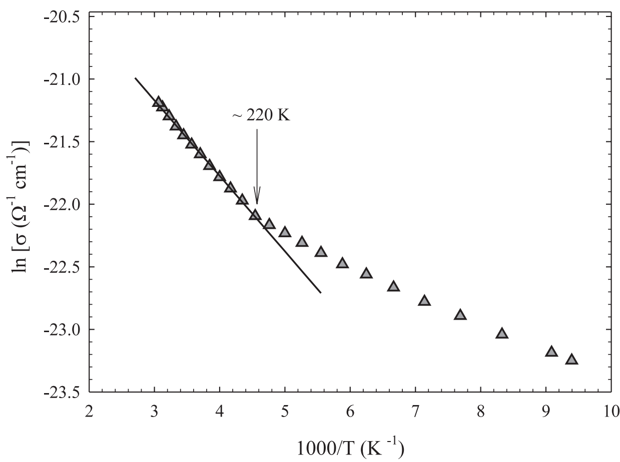

Fig. 5. Temperature dependence of the conductivity for a-Si:H film plotted as $\ln\sigma$ vs $1000/T$ at whole temperature range. Solid triangles represent the experimental points. The line is least square fit to the data for $T > 220$ K. A closer inspection reveals that the linearity does not continue below 220 K. The temperature of deviation from the linearity is marked as 220 K.

temperature ranges. These two mechanisms may be distinguished experimentally by operating in appropriate temperature ranges. The conductivity is found to increase with the increase in temperature and the increase is observed to be very gradual and small for temperatures below about 220 K.

For the high temperature range ($T > 220$ K), we have succeed to fit the conductivity data of the film to the Arrhenius plot. This suggests a simple thermal activation process that dominates the electrical conduction in the film in temperature range of $T > 220$ K. Our sample is very resistive and its activation energy is very low when compared with the values reported in literature.[5–9] This may indicate that the Arrhenius behavior of conductivity (Fig. 5) essentially represents the NNH conduction mechanism for $T > 220$ K.[15]

In the NNH conduction, electron with an activation energy (W) hops to the nearest neighboring empty site. This activation energy has much smaller value as compared to the energy required for thermally activated band conduction.[15] In the presence of NNH mechanism in a material, the condition of $\lambda \gg 1$ should be satisfied.[16,17] If $\lambda \rightarrow 1$, the system exhibits a metallic behavior.[16,17] λ was defined by Mott and Twose[16] as the ratio r/a_{B}^{*}, where a_{B}^{*} is the effective Bohr radius that is given with relation:

$$a_{\mathrm{B}}^{*} = \frac{4\pi\varepsilon_0\varepsilon\hbar^2}{m^{*}e^2}. \tag{4}$$

Here, ε_0 is the permittivity of vacuum, e is the electron charge and $\hbar$ is Planck's constant. Using the values of effective mass of $m^{*} = 0.4\,m_0$[13] and static dielectric constant of $\varepsilon = 11.9$ which is deduced from optical absorption data of the investigated sample, a_{B}^{*} can be calculated as 1.59 nm. With the value of $N_{\mathrm{d}} = 9.6 \times 10^{16}\,\mathrm{cm}^{-3}$, the NNH distance, r, is obtained as 13.54 nm with using the relation:

$$r = \left(\frac{4\pi N_{\mathrm{d}}}{3}\right)^{1/3}. \tag{5}$$

Then, we can easily obtain the parameter λ using the relation of $\lambda = r/a_{\mathrm{B}}^{*}$ as 8.52 with the known values of a_{B}^{*} and r. The requirement for the NNH, $\lambda \gg 1$ is clearly satisfied for the investigated sample.

In the NNH regime, temperature dependence of conductivity can be derived as following. For the localized states with an energy separation W and the NNH distance r, the hopping probability can be written as[13]

$$P_{\mathrm{hop}} = \nu_{\mathrm{ph}} \exp\left(-\frac{2r}{\xi} - \frac{W}{k_{\mathrm{B}}T}\right), \tag{6}$$

where ν_{ph} is the phonon frequency associated with hopping process, k_{B} is Boltzmann's constant, and ξ is localization length. The diffusion coefficient D_{hop} for hopping is given by[13]

$$D_{\mathrm{hop}} = \frac{P_{\mathrm{hop}} r^2}{6}. \tag{7}$$

Using the Einstein relation, the conductivity can be written as

$$\sigma = e^2 D_{\mathrm{hop}} g(E). \tag{8}$$

Combining eqs. (6)–(8), the temperature dependence of conductivity in the NNH regime is found as[13]

$$\sigma = \frac{1}{6} g(E)\nu_{\mathrm{ph}} e^2 r^2 \exp\left(-\frac{2r}{\xi} - \frac{W}{k_{\mathrm{B}}T}\right), \tag{9}$$

$$\sigma = \sigma_3 \exp\left(-\frac{W}{k_{\mathrm{B}}T}\right), \tag{10}$$

where $g(E)$ is the density of states (DOS). From eq. (10), the value of W is obtained as 55 meV for the investigated sample.

A further decrement in temperature ($T < 220$ K) leads to a deviation from the linearity as shown in Fig. 5. This type of behavior has been observed in many amorphous semiconductors and it is a characteristic of the change in conduction mechanism from thermally activated conduction to the VRH conduction.[5–9] According to Mott,[3] electron hopping between nearest neighbor sites is not always favored at low temperatures as the levels may be significantly different in energy. It is possible that electrons can prefer to move to a more energetically similar remote site. In this regime, the following conduction law is expected for the variation of the conductivity of amorphous disordered systems:[3,4]

$$\sigma = \sigma_0 \exp\left(-\frac{T_0}{T}\right)^{s}. \tag{11}$$

Here, σ_0 is the pre-exponential factor and, T_0 is a characteristic temperature. When the VRH mechanism dominates the conduction, the condition $0 < s < 1$ is fulfilled. If the density of states around the Fermi level assumed to be constant, s becomes $s = 1/4$ (Mott VRH). On the other hand, if there is a gap at the Fermi level, the VRH conduction model is expressed with $s = 1/2$ in eq. (11) (ES VRH).[3,4] Also, the value of $s = 1$ in eq. (11) corresponds to the NNH mechanism.

In order to achieve deeper understanding the low temperature electrical conduction properties of the investigated sample, the variation in the electrical conductivity as a function of $T^{-1/2}$ and of $T^{-1/4}$ is shown in Fig. 6 and the

 © 2009 The Japan Society of Applied Physics

Person-to-person distribution (up to 10 persons) by the author only. Not permitted for publication for institutional repositories or on personal Web sites.

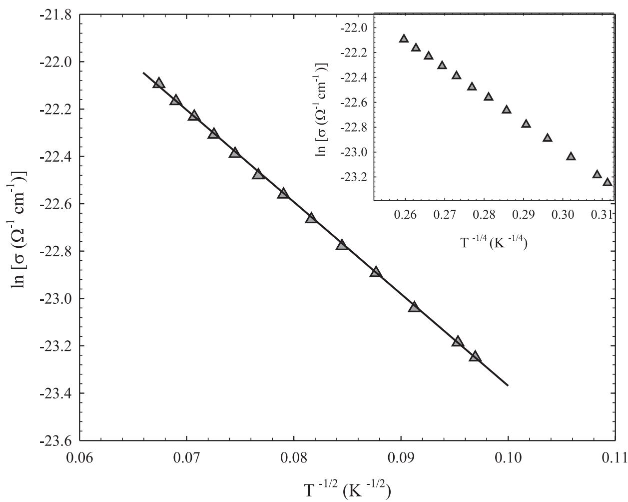

Fig. 6. Temperature dependence of the conductivity for a-Si:H film plotted in the ES VRH formalism for $T < 220$ K. Solid triangles represent the experimental points. The solid line represents the fits according to the ES VRH model. The plot is redrawn according to the Mott VRH model in the inset, which is discussed in text.

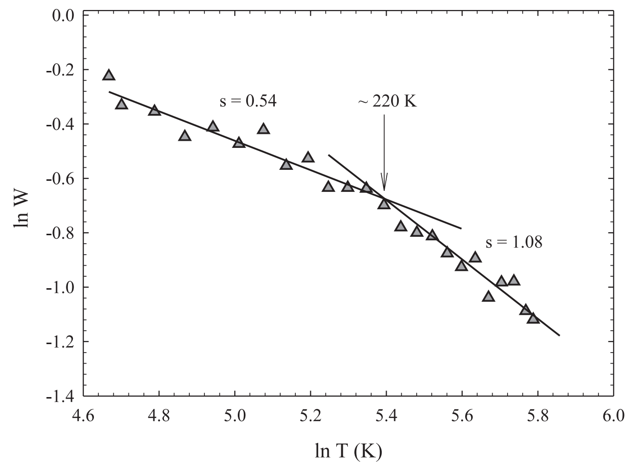

Fig. 7. Plot of ln[$W(T)$] vs ln T for a-Si:H film, calculated from experimental $\sigma(T)$ at whole temperature range. Solid triangles and solid lines represent the experimental points and the best fits with eq. (13), respectively. We find that there are two types of conduction mechanisms contributing to the conductivity in different temperature ranges, which is discussed in text. A fit of eq. (13) to data yields the hopping exponents of $s = 1.08$ and 0.54 for $T > 220$ K and for $T < 220$ K, respectively. The crossover temperature is marked as 220 K.

inset of Fig. 6, respectively. It is found that the temperature dependent conductivity can be fairly good fitted when the scale of T^{-1} changes place with $T^{-1/2}$ or $T^{-1/4}$ for $T < 220$ K. However, it is hard to decide whether the NNH or the ES VRH and the Mott VRH are dominant conduction mechanism for $T < 220$ K. To determine accurately the value of s in eq. (11), the most appropriate way is to analyze the conductivity versus temperature data using the approach of Zabrodskii and Zinoveva.[18] Hence, by defining the parameter $W(T)$ with relation:

$$W(T) = \frac{d \ln \sigma(T)}{d \ln T}, \tag{12}$$

we get from the eq. (11),

$$W(T) = \ln s + s \ln T_0 - s \ln T. \tag{13}$$

$W(T)$ can be also used to determine metallic and insulating behavior of the conductivity. When the slope of ln[$W(T)$] vs ln T is negative, that is, W increases as T decreases, the system is in the insulating side of metal–insulator transition. The positive slope of the W plot indicates that the system can be in the metallic regime.

Figure 7 shows ln[$W(T)$] vs ln T. $W(T)$ decreases with increasing temperature. By making a linear regression fit of the ln[$W(T)$] vs ln T data in the whole temperature range, the hopping exponent $s = 1.080 \pm 0.136$ and 0.540 ± 0.045 are obtained for $T > 220$ K and for $T < 220$ K, respectively. This clearly indicates that the conduction in the investigated sample is due to the NNH conduction for $T > 220$ K and the ES VRH conduction for $T < 220$ K, respectively.

The plot of $\ln \sigma$ vs $T^{-1/2}$ in Fig. 6 is found to be linear at low temperatures ($T < 220$ K). The $\chi^2 = 0.998$ (χ is the correlation coefficient) is obtained, which indicates a satisfactory fit. Again, this confirms that the conduction in the investigated sample is governed by the ES VRH ($T^{-1/2}$ law) conductivity for $T < 220$ K. In eq. (11), the value of T_0 is derived as 2180 K from the slope of the $\ln \sigma$ vs $T^{-1/2}$ plot in Fig. 6. This value of T_0 is appropriate for disorder or amorphous materials.[8] We can evaluate several other hopping parameters, e.g., hopping distance, hopping energy, etc. with the known value of T_0. The temperature dependent hopping distance (R_{hop}) is given by[4,19]

$$R_{hop} = \frac{3^{1/6}}{2^{5/6}\beta^{1/2}}\left(\frac{T}{T_0}\right)^{1/2}\xi, \tag{14}$$

and the hopping energy (Δ_{hop}) is defined as[4,19]

$$\Delta_{hop} = \frac{6^{1/6}}{\beta^{1/2}} k_B T\left(\frac{T_0}{T}\right)^{1/2}, \tag{15}$$

where $\beta = 2.8$.[4] Since the DOS, $g(E)$, has to be parabolic about the Fermi level in the ES VRH regime, then one can obtain

$$g(E) = g_2(E - E_F)^2, \tag{16}$$

where E_F is Fermi energy level and g_2 can be expressed as[19]

$$g_2 = \frac{3^8 \pi^2 \varepsilon^3 \varepsilon_0^3}{2^5 e^6}. \tag{17}$$

Then, localization length (ξ), which is given in eq. (9), can be calculated using the following relation,[19]

$$\xi^{-1} = \frac{k_B T_0 (\pi g_2)^{1/3}}{10.5}. \tag{18}$$

In the ES VRH regime, the long-range Coulomb interaction between the localized state electrons cause in the DOS to tend to zero in the vicinity of Fermi energy, which results in a soft energy gap, i.e., Coulomb gap corresponding to the parabolic DOS. It is assumed that the DOS would level off when $g(E) = g_0$. T_0 is related to Coulomb gap energy (Δ_C) and DOS (g_0) as[4,19,20]

$$\Delta_C = 0.5 k_B (T_0 T_c)^{1/2}, \tag{19}$$

$$g_0 = \frac{3^8 \pi^2 k_B^2 \varepsilon^3 \varepsilon_0^3}{2^9 e^6}(T_0 T_c). \tag{20}$$

© 2009 The Japan Society of Applied Physics

Person-to-person distribution (up to 10 persons) by the author only. Not permitted for publication for institutional repositories or on personal Web sites.

To extract the value of localization length (ξ), we used the value of $T_0 = 2180$ K and then it is found to be 4.54 nm. Here, ξ is of the order 1 nm, which is consistent with the expected magnitude in the VRH regime.[3,4)]

In order to determine the validity of either of NNH or VRH model, a basic criterion was suggested by Mott and Davis.[3)] If $r/\xi < W/k_B T$, the VRH conduction model is valid, and if $r/\xi > W/k_B T$, the NNH conduction model is valid. Thus, according to the hopping picture, one would expect a crossover in the temperature dependent conductivity. Above the crossover temperature (T_c), electron transport is via the NNH, whereas below T_c, electrons may optimize their paths by using the VRH, results a weaker temperature dependence of conductivity. Therefore the criterion, $r/\xi = W/k_B T$, naturally gives the crossover temperature. Utilizing the quantities W, r, and ξ, the value of the T_c is obtained as 214 K. The fact that the activation energies lead to a $r/\xi < W/k_B T$, a conclusion that conduction is due to the VRH is justified for $T < 214$ K, while conduction is the NNH for $T > 214$ K due to $r/\xi > W/k_B T$. The theoretical value of 214 K is in excellent qualitative agreement with the experimental value of 220 K determined by fitting the data (Fig. 7).

Using the value of T_0 and ξ, the value of R_{hop} at 150 K and the corresponding value of Δ_{hop} are obtained as 6.97 nm and 39.8 meV, respectively. For our sample, we have taken the crossover temperature as $T_c = 220$ K since crossover from the NNH to the ES VRH was observed at about this temperature (Fig. 7). By using the values of T_0, we can also calculate the values of Δ_C and g_0 as 29.86 meV and 1.32×10^{20} eV^{-1} cm^{-3}, respectively. The obtained VRH parameters for the investigated sample are in agreement with the expected range of values in the VRH regime.[3,4)] Also, these results present a fair agreement with several reported by some researchers[5–9,21,22)] that found the VRH is the predominant transport mechanism for both amorphous silicon and variety of disordered systems. Therefore, the calculated hopping parameters have physically plausible values.

A good fit of the measured data is essential but not sufficient criterion for applicability of the ES VRH model. The hopping parameters should satisfy the ES VRH model's requirements. To use three dimensional (3D) ES VRH model in the investigated sample, the following criteria are to be satisfied:[4)]

$$\Delta_{hop} \geq k_B T, \quad (21)$$

$$d \gg R_{hop}, \quad (22)$$

$$R_{hop}/\xi \geq 1, \quad (23)$$

$$\Delta_C > \Delta_{hop}. \quad (24)$$

From the values of the different parameters evaluated for our sample that the first three criteria are satisfied, i.e., the hopping energy (Δ_{hop}) is always greater than $k_B T$, the hopping distance (R_{hop}) is considerably less than the thickness ($d = 1.94$ µm) of the sample and the ratio of the hopping distance (R_{hop}) to the localization length (ξ) is greater than one. However, in the ES VRH regime, the last criterion is not fulfilled. A small value of the Coulomb gap is due to the large value of the dielectric constant of amorphous silicon. Such a situation has also been reported for various disordered systems that have high dielectric constant.[8,21)]

4. Conclusions

We investigated optical and electrical properties of the a-Si:H film which was prepared by hot wire method, using the transmittance and conductivity measurements. The dielectric constant of a-Si:H film was determined from the transmittance measurement as 11.9, which is in well agreement with the generally accepted value. In the studied temperature range, the temperature dependence of conductivity was satisfactorily explained by the NNH and ES VRH models. The obtained hopping parameters are reasonable agreement with theoretical predictions. We obtained a transition from NNH to ES VRH. An excellent agreement between the theoretical ($T \approx 214$ K) and the experimental ($T \approx 220$ K) values of transition temperature was obtained.

Acknowledgements

The authors would like to thank Dr. B. Schröder and his group member for the laboratory facilities and help of the preparation of a-Si:H films.

1) D. Knipp, R. A. Street, H. Stiebig, M. Krause, J. P. Lu, S. Ready, and J. Ho: IEEE Trans. Electron Devices **53** (2006) 1551.
2) P. Servati, D. Striakhilev, and A. Nathan: IEEE Trans. Electron Devices **50** (2003) 2227.
3) N. F. Mott and E. A. Davis: *Electronic Properties in Non-Crystalline Materials* (Clarendon Press, Oxford, U.K., 1971).
4) A. L. Efros and B. I. Shklovskii: *Electronic Properties of Doped Semiconductors* (Springer, Berlin, 1984).
5) Y. Ohmura, M. Takahashi, M. Suzuki, A. Emura, N. Sakamoto, T. Meguro, and Y. Yamamoto: Phys. Status Solidi B **235** (2003) 111.
6) S. K. Sharma, P. Sagar, H. Gupta, R. Kumar, and R. M. Mehra: Solid-State Electron. **51** (2007) 1124.
7) I. P. Zvyagin, I. A. Kurova, and N. N. Ormont: Phys. Status Solidi C **1** (2004) 101.
8) A. I. Yakimov, T. Wright, C. J. Adkins, and A. V. Dvurechenskii: Phys. Rev. B **51** (1995) 16549.
9) A. J. Lewis: Phys. Rev. B **14** (1976) 658.
10) M. F. Thorpe and D. Weaire: Phys. Rev. Lett. **27** (1971) 1581.
11) R. Svanepoel: J. Phys. E **16** (1983) 1214.
12) W. G. Spitzer and H. Y. Fan: Phys. Rev. **106** (1957) 882.
13) R. A. Street: *Hydrogenated Amorphous Silicon* (Cambridge University Press, Cambridge, U.K., 1991).
14) C. T. Sah: *Fundamentals of Solid-State Electronics* (World Scientific, Singapore, 1993).
15) A. Miller and E. Abrahamas: Phys. Rev. **120** (1960) 745.
16) N. F. Mott and W. D. Twose: Adv. Phys. **10** (1961) 107.
17) A. Hausmann and W. Teuerle: Z. Phys. A **257** (1972) 299.
18) A. G. Zabrodskii and K. N. Zinoveva: Sov. Phys. JETP **59** (1984) 425.
19) C. J. Adkins: J. Phys.: Condens. Matter **1** (1989) 1253.
20) A. N. Ionov, I. S. Shlimak, and M. N. Matveev: Solid State Commun. **47** (1983) 763.
21) A. Yildiz, S. B. Lisesivdin, M. Kasap, and D. Mardare: J. Non-Cryst. Solids **354** (2008) 4944.
22) A. Yildiz, S. B. Lisesivdin, M. Kasap, and D. Mardare: Physica B **404** (2009) 1423.

 © 2009 The Japan Society of Applied Physics

View publication stats